Appl Phys B (2009) 97: 639–643
DOI 10.1007/s00340-009-3755-x

Applied Physics B
Lasers and Optics

High-efficiency, high-power, diode-pumped continuous-wave Tm:$YAlO_3$ slab lasers

X. Cheng · F. Chen · G. Zhao · J. Xu

Received: 9 March 2009 / Revised version: 20 August 2009 / Published online: 2 October 2009

Abstract We report diode end-pumped continuous-wave Tm:$YAlO_3$ slab lasers with high power and high efficiency. At room temperature, *b*-cut Tm:$YAlO_3$ slabs with doping concentrations of 1, 4 and 5 at.% pumped by fiber-coupled and fast-axis collimated laser diodes with different wavelengths are compared. Tm:$YAlO_3$ slab lasers of 4 at.% doping concentrations have the highest optical-to-optical efficiency. When pumped with fiber-coupled and fast-axis collimated laser diodes, the maximum output powers are 11 W and 15 W, corresponding to a slope efficiency of 52% and 40%, respectively.

PACS 42.55.Rz · 42.55.Xi · 42.60.Pk

1 Introduction

Two micrometer lasers have been an important research field of solid-state lasers because of their particular characters. Firstly, there being strong absorption by liquid water, 2-μm lasers are eye-safe light sources that have been widely used in surgery and dentistry. Secondly, 2-μm lasers have an important application in remote sensing and optical communications, especially in coherent Doppler LIDAR and water vapor parabolic surface differential absorption laser radar system. Thirdly, high-power 2-μm lasers can be used as an efficient pump source for Mid-IR 3∼5-μm optical parametric oscillators (OPO) [1–4]. Because of the long fluorescence lifetime, the high quantum efficiency introduced by cross relaxation mechanism, and the ability to be pumped directly by commercial laser diodes (LD), the Tm-doped solid-state laser, such as Tm:YAG, Tm:YLF, Tm:$LiLuF_4$, and Tm:KLu $(WO4)_2$, has been studied and reported recently [5–10]. Except for the similar thermal and mechanical properties to Tm:YAG crystal, Tm:$YAlO_3$ is a natural birefringence crystal to excite polarized light without external polarizer. Furthermore, the emission cross section of $YAlO_3$ is twice as high as that of YAG crystal [11]. Although many research results of Tm:$YAlO_3$ have been reported in recent years [12–14], detailed research to get higher output power with high efficiency is still needed.

In this paper, diode end-pumped Tm:$YAlO_3$ slab lasers of different doping concentrations have been investigated. Both fiber-coupled and fast-axis collimated LDs with different wavelengths are used as pump sources. The slab crystal has superior thermal removing ability than rod crystal, while the aspect ratio is greater than 2 and can easily be used to power scaling. With a thin slab structure, 148 W continuous-wave output power has been obtained from 2 at.% Tm:YLF crystal [15, 16]. So the Tm:$YAlO_3$ crystal has been designed with thin slab structure and the thickness of the slabs is only 1 mm, which is similar to the Nd:YAG crystal we studied previously. The experimental results show that whether pumped by fiber-coupled or fast-axis collimated LD, Tm:$YAlO_3$ slab laser of 4 at.% doping concentration has the highest optical efficiency. At room temperature, when the fiber-coupled LD is used as the pump source, the maximum output power of 4 at.% Tm:$YAlO_3$ is 11 W at 24 W absorbed pump power. While using fast-axis collimated LD, we got 15 W from 4 at.% Tm:$YAlO_3$ laser with 44.5 W absorbed pump power.

X. Cheng (✉) · F. Chen · G. Zhao · J. Xu
The Novel Laser Technique and Application System Laboratory, Shanghai Institute of Optics and Fine Mechanics, Chinese Academy of Science, Shanghai, 201800, China
e-mail: xjcheng@siom.ac.cn
Fax: +86-21-69918507

2 Spectrum

Because of anisotropy, the absorption coefficient α of Tm:$YAlO_3$ crystal varies when the pump light propagates along the a-, b- and c-axis. The absorption spectrum was measured by a spectrophotometer (JASCO V-570) and the absorption coefficient was calculated by the Beer-Lambert law. As shown in Fig. 1, we can find while the pump light propagates on c-axis, the maximum absorption coefficient is $\alpha = 6.23\ \mathrm{cm}^{-1}$ for the pump wavelength at 795 nm. When the pump light propagates along b-axis, the central absorption wavelength is also near 795 nm and the absorption coefficient is $4.36\ \mathrm{cm}^{-1}$. But for the a-axis, there are two absorption peaks, one is at 794 nm with $\alpha = 4.25\ \mathrm{cm}^{-1}$ and the other is at 800 nm with $\alpha = 3.99\ \mathrm{cm}^{-1}$. According to these absorption coefficients, more than 90% pump light can be absorbed with a 4- and 6-mm long crystal, while $\alpha = 6.23$ and $\alpha = 4.36\ \mathrm{cm}^{-1}$, respectively. In order to get high-power laser output, a longer slab for a better heat removal is necessary. Due to the effects of cross-relaxation and concentration quenching, a Tm:$YAlO_3$ crystal with doping concentration around 3∼5 at.% gives the higher slope efficiency. Thus, it is not appreciated to lengthen the slab by choosing a low doping concentration as that commonly does in Nd:YAG slab lasers. We cut Tm:$YAlO_3$ crystal along the b-axis and shift the pump wavelength from the absorption peak. In such a case, we can use a longer slab to hold high pump power and keep high efficiency in the meantime.

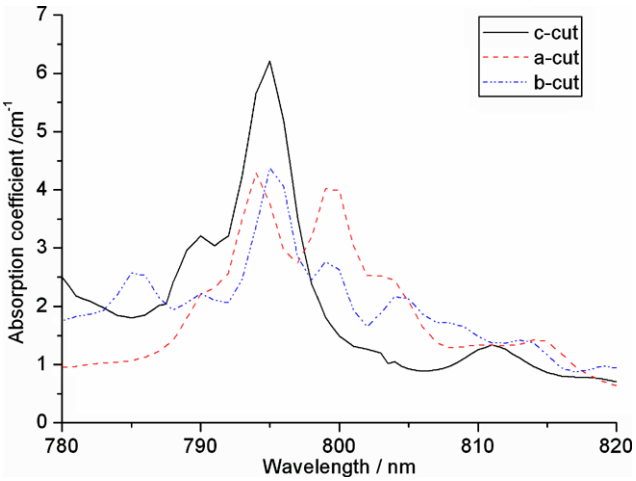

Fig. 1 Absorption spectrum of 4 at.% Tm:$YAlO_3$ crystal being cut along a-, b- and c-axis respectively

The thermal conductivity of Tm:$YAlO_3$ crystals also depends on doping concentration and axis direction. Thermal conductivity k was got by measuring the thermal diffusivity β and calculated from $k = \beta C \rho$ in which C is the ratio of specific heat and ρ is the density. At room temperature, the thermal conductivity drops from 9.96 to 5.79 $\mathrm{W \cdot m^{-1} \cdot K^{-1}}$, while the doping concentration increases from 1.0 to 5.0 at.% along the b-axis direction. For the same doping concentration, the thermal conductivity varies in different axis directions. The conductivity along a-, b- and c-axis are 5.5, 6.29 and 5.71 $\mathrm{W \cdot m^{-1} \cdot K^{-1}}$ for 4 at.% doped Tm:$YAlO_3$ crystal. Heat removal is most uniform in the b-cut crystal, which is beneficial to good output beam quality for high-power slab lasers.

3 Laser experiments and results

Table 1 gives the related parameters used in the laser experiments. The slabs dimension are $1 \times 5 \times 12$ mm, $1 \times 5 \times 6$ mm and $1 \times 5 \times 6$ mm corresponding to the doping concentration of 1 at.%, 4 at.% and 5 at.%, respectively. All the slabs are b-cut with 1 mm thickness (a-axis) and 5 mm width (c-axis) and end-pumped by LD. Figure 2 shows the experimental

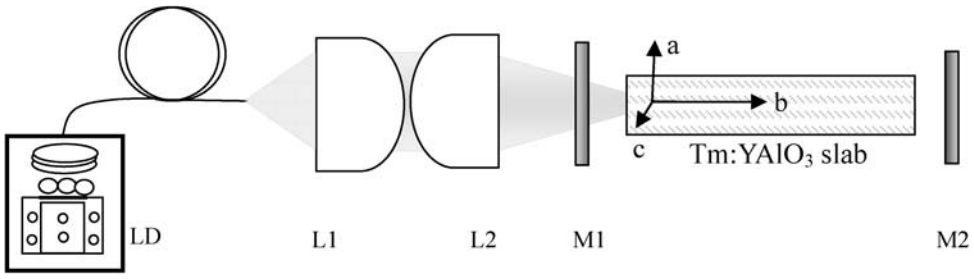

Fig. 2 Scheme of the Tm:$YAlO_3$ laser pumped by fiber-coupled LD

Table 1 Parameters used in the laser experiments

Tm:$YAlO_3$		Central wavelength of pump LDs (LD)	
Doping concentration (at.%)	Dimension (mm)	Fiber-coupled LD	Fast-axis collimated LD
1	$1 \times 5 \times 12$	795 nm, 24°C	791.5 nm, 24°C
4	$1 \times 5 \times 6$		
5	$1 \times 5 \times 6$		

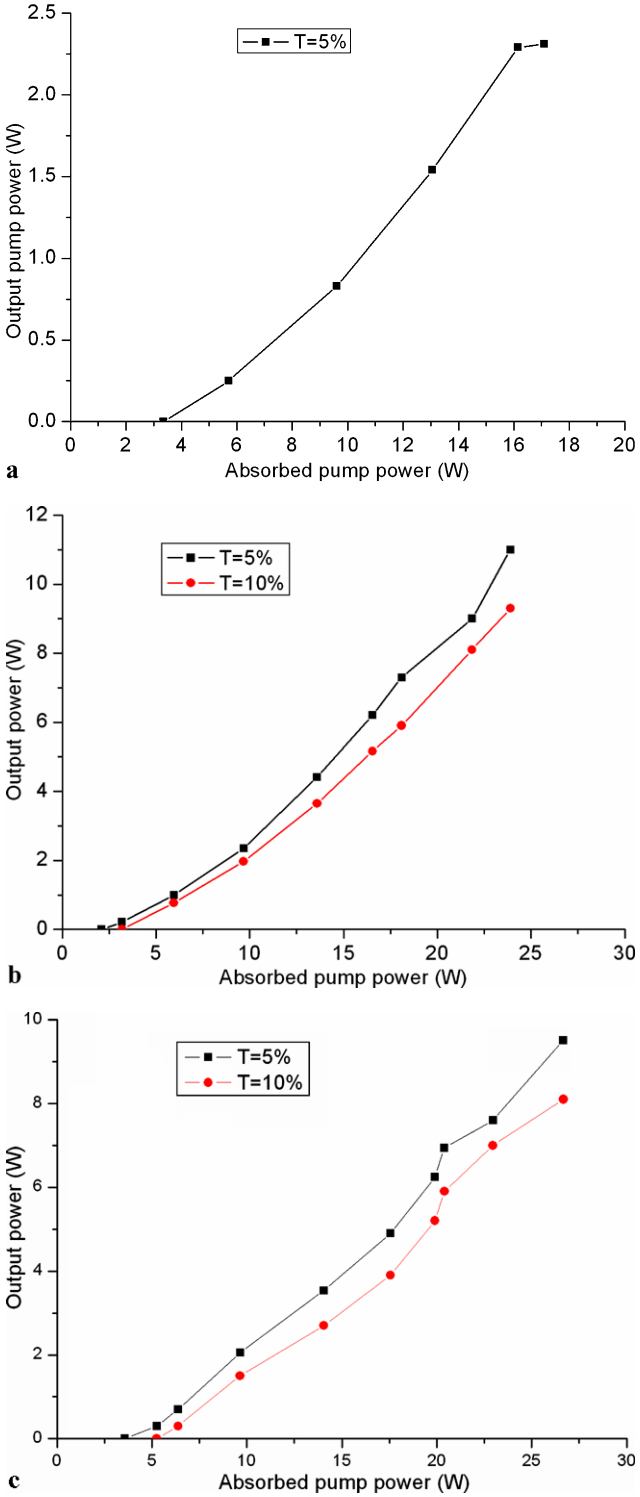

Fig. 3 Output power versus absorbed pump power with fiber-coupled LD: (**a**) 1 at.%; (**b**) 4 at.%; (**c**) 5 at.%

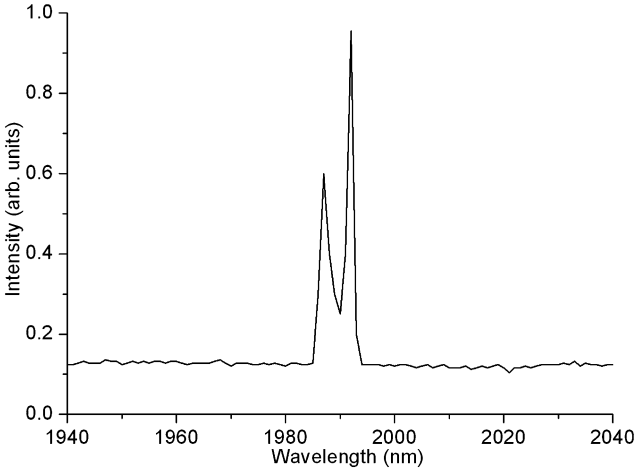

Fig. 4 Laser spectrum of Tm:$YAlO_3$ laser with the output coupling of 5% and the doping concentration of 4 at.%

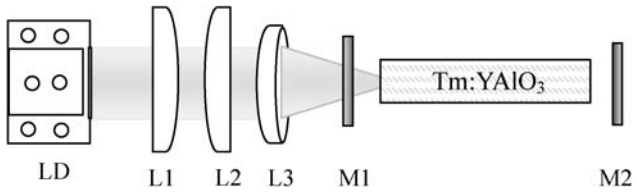

Fig. 5 Scheme of the Tm:$YAlO_3$ laser pumped by Fast-axis collimated LD

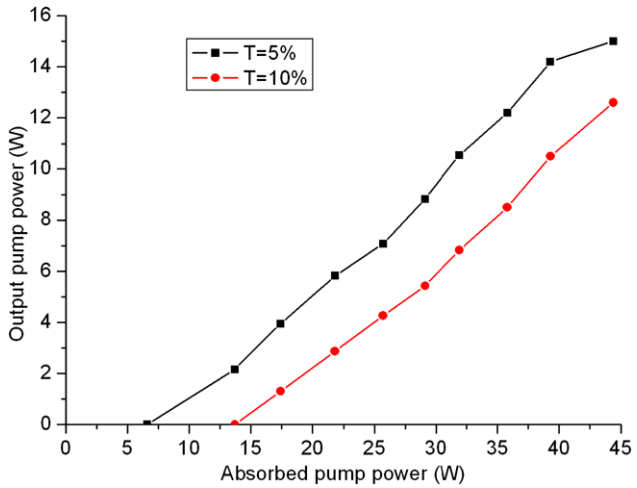

Fig. 6 Output power versus absorbed pump power with fast-axis collimated LD for 4 at.% Tm:$YAlO_3$ slab laser

scheme of the Tm:$YAlO_3$ slab laser, which is end-pumped by the fiber-coupled LD. The LD module can provide 30 W CW power with a fiber diameter of 400 μm and a numerical aperture of 0.22. The central wavelength of the LD is 795 nm with the cooling water temperature of 24°C. The pump beam is shaped by the two same plano-convex spherical lenses, whose focal lengths are 90 mm. The pump waist of 1.0 mm in diameter was positioned on the rear facet of the Tm:$YAlO_3$ slab. A compact plane-parallel cavity consisting of mirrors M1 and M2 was used for the Tm:$YAlO_3$ slab laser. The rear mirror M1 is AR-coated at 790 ± 15 nm and HR-coated at 2000 ± 50 nm. The output coupler M2

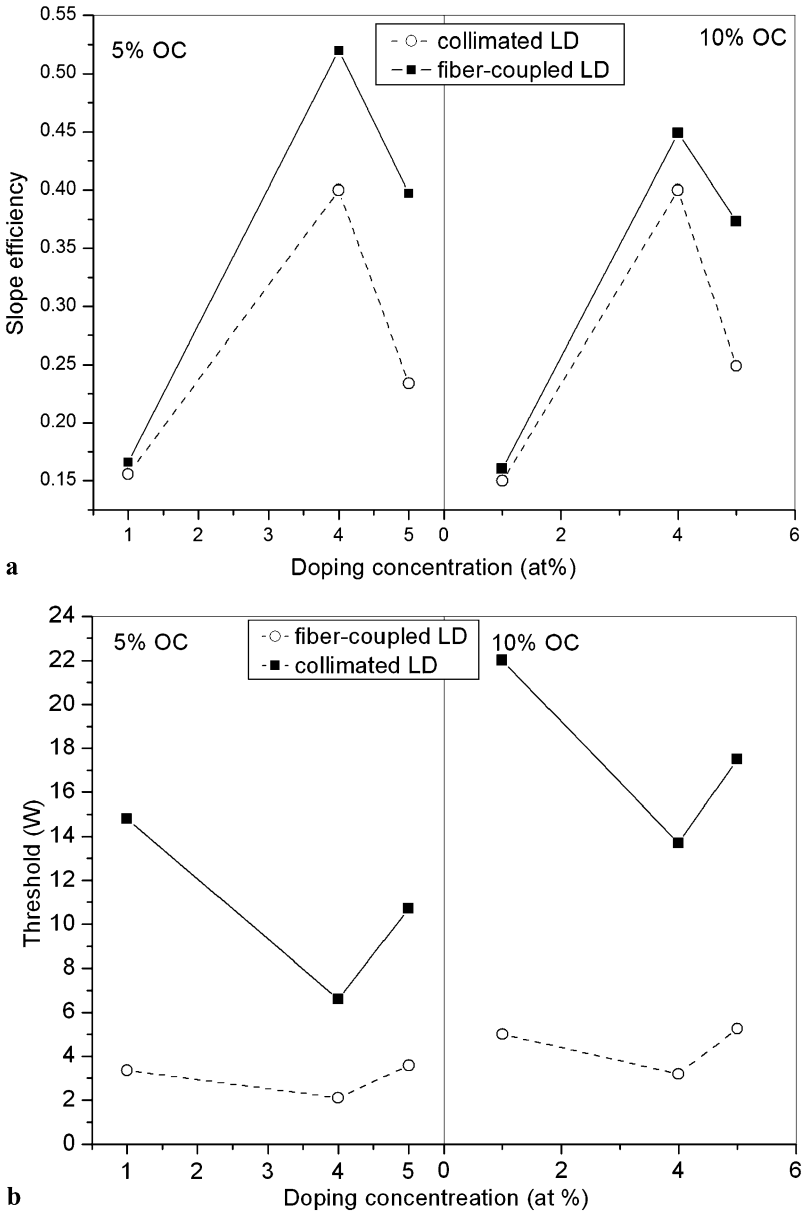

Fig. 7 Slope efficiency and pump threshold of Tm:$YAlO_3$ slab lasers for various doping concentrations

is coated at 2000 ± 50 nm with the reflectivity of 95% or 90%. Two big surfaces of Tm:$YAlO_3$ slab are wrapped in indium foil and water-cooled by a copper micro channel heat-sink. The temperature of cooling water was set at 17°C. Because the wavelength of LD red-shifts by 0.3 nm/°C, the absorption coefficient is less than the maximum value indicated in Fig. 1.

The output power of the Tm:$YAlO_3$ slab laser with the fiber-coupled LD is shown in Fig. 3. The maximum optical efficiency was obtained in the 4 at.% doping concentration Tm:$YAlO_3$. This coincides with the experiment results where the Tm:$YAlO_3$ crystal is pumped along the *c*-axis [11–13]. For 4 at.% Tm:$YAlO_3$ slab, the output power are 11 W and 9.3 W at the 24 W absorbed pump power with the output coupling of 5% and 10%, respectively, corresponding to the slope efficiency of 52% and 45%. For the lower doping concentration, the cross-relaxation between ions is insufficient and the role of two-for-one mechanism is not filled. The slope efficiency from 1 at.% Tm:$YAlO_3$ is only 16%. However, for the higher doping concentration, fluorescence quenching becomes more serious and the slope efficiency is also reduced. For 5 at.% Tm:$YAlO_3$ slab, even the absorption of pump light is increased about 11%, and the final output power is 9.5 W, less than that of 4 at.% crystal.

Figure 4 shows the output laser spectrum of the Tm:$YAlO_3$ slab laser with the output coupling of 5% and the doping concentration of 4 at.%. The central laser wavelength of *b*-cut Tm:$YAlO_3$ is 1991 nm with the 4 at.% doping concentration. Several peaks can be found in the spectra resulting from broad emission of Tm^{3+} ions. The laser spec-

tra including all peaks are between 1980 and 1996 nm for all doping concentrations. The central laser wavelength of 1 at.% and 5 at.% doping concentrations, *b*-cut Tm:$YAlO_3$ are 1992 nm and 1988 nm respectively.

Figure 5 shows the scheme of the Tm:$YAlO_3$ laser which is end-pumped by fast-axis collimated LD. The central wavelength of the LD is 791.5 nm at a temperature of 24°C. The pump delivery system for the fast-axis collimated LD is built up by two plano-convex cylindrical lenses and one plano-convex spherical lens, whose focal lengths are all 90 mm. The system can attain delivery at about 65 W CW power with the size of 0.8×2 mm to the Tm:$YAlO_3$ slab. The average pumping intensity is almost the same as that pumped by fiber-coupled LD. More pump power can be launched into the slab by enlarging the pump beam width.

The output power of the Tm:$YAlO_3$ slab laser with fast-axis collimated LD is shown in Fig. 6. The behavior is similar as the case pumped by fiber-coupled LD. The maximum output power is also got from 4 at.% Tm:$YAlO_3$ crystal. The output power of 15 W and the slope efficiency of 40% are achieved with the output coupling of 5%.

The slope efficiencies and threshold of pumping with fiber-coupled and collimated LD are compared in Fig. 7. The lasers pumping with fiber-coupled LD have higher slope efficiency because of the overlap between the pump and laser beams. With pumping by fiber-coupled LD, the overlap is calculated to be 90%. In contrast, with pumping by collimated LD, the overlap reduces to 78%. Taking into account the difference of the overlap, the slope efficiency is influenced slightly by the pumping wavelength. As shown in Fig. 7, pumped with fast-axis collimated LD, the threshold is >3 times higher than that pumped by fiber-coupled LD. Considering that the pump area is two times larger, the pump intensity at threshold is >1.5 times higher with the pumping of fast-axis collimated LD. One possibility is that the absorption cross section at 791.5 nm is lower, and a higher pump intensity is needed to reach the threshold.

Whether pumped with fiber-coupled or collimated LD, the Tm:$YAlO_3$ crystal at 4 at.% has a higher sloping efficiency and lower threshold than 1 at.% and 5 at.%. Which matches to the calculation result that Tm:$YAlO_3$ crystal at 4 at.% has the larger emission cross section and longer lifetime of the $^3F_4$ energy level at room temperature. With higher doping concentration, the effect of upconversion becomes more and more serious, which leads to higher threshold and lower sloping efficiency [17]. Furthermore, concentration quenching caused by clusters of thulium ions will also aggravate at increasing doping concentration.

4 Conclusion

In conclusion, we demonstrated high-power, high-efficiency, continuous-wave, room temperature Tm:$YAlO_3$ slab lasers with diode end pumping. Different doping concentrations of *b*-cut Tm:$YAlO_3$ slab lasers pumped by different wavelength LDs are compared. The maximum output power values are 11 W and 15 W with the slope efficiency of 52% and 40%, while the pump source are fiber-coupled and fast-axis collimated LD, respectively. The experimental results show that *b*-cut Tm:$YAlO_3$ crystal slab pumped by a shifted wavelength is an effective configuration for 2-μm lasers and 4 at.% is a properly doping concentration for *b*-cut Tm:$YAlO_3$ crystal lasers operated at room temperature.

Acknowledgements The authors acknowledge researchers from the Laser & Optoelectronic Functional Material R&D Center of Shanghai Institute of Optics and Fine Mechanics, Chinese Academy of Science for their support with the Tm:$YAlO_3$ crystals. The work is partially supported by the Natural Science Foundation of China under contract 60678016.

References

1. W. Koechner, *Solid-state laser engineering*, 5th edn. (Springer, Berlin, 1999). Chap. 2
2. P.J.M. Suni, S.W. Henderson, Opt. Lett. **16**, 817 (1991)
3. I.F. Elder, M.J.P. Payne, Opt. Commun. **145**, 329 (1998)
4. T.J. Carrig, A.K. Hankla, G.J. Wagner, C.B. Rawle, I.T.M. Kinnie, Laser radar technology and applications VII. Proc. SPIE **4723**, 147 (2002)
5. K.S. Lai, P.B. Phua, R.F. Wu, Y.L. Lim, E. Lau, S.W. Toh, B.T. Toh, A. Chng, Opt. Lett. **25**, 1591 (2000)
6. M. Schellhorn, Appl. Phys. B **91**, 71 (2008)
7. A. Dergachev, K. Wall, P. Moulton, Adv. Solid State Lasers **68**, 343 (2002)
8. N. Coluccelli, G. Galzerano, P. Laporta, F. Cornacchia, D. Parisi, M. Tonelli, Opt. Lett. **32**, 2040 (2007)
9. X. Cheng, S. Zhang, J. Xu, H. Peng, Y. Hang, Opt. Express **17**, 14895 (2009)
10. V. Petrov, L. Junhai, G. Miguel, V. Gregorio, P. Cinta, G. Uwe, A. Magdalena, D. Francesc, SPIE **6216**, 162 (2006)
11. S.A. Payne, L.L. Chase, L.K. Smith, W.L. Kway, W.F. Krupke, IEEE J. Quantum Electron. **QE-28**, 2619 (1992)
12. T. Thevar, N.P. Barnes, Appl. Opt. **45**, 3352 (2006)
13. S.S. Cai, J. Kong, B. Wu, Y.H. Shen, G.J. Zhao, Y.H. Zong, J. Xu, Appl. Phys. B **90**, 133 (2008)
14. A.C. Sullivan, G.J. Wagner, D. Gwin, R.C. Stoneman, A.I.R. Malm, in *Advanced Solid-State Photonics (ASSP)*, paper WA7 (2004)
15. S. So, J.I. Mackenzie, D.P. Shepherd, W.A. Clarkson, J.G. Betterton, E.K. Gorton, Appl. Phys. B **84**, 389 (2006)
16. M. Schellhorn, S. Ngcobo, C. Bollig, Appl. Phys. B **94**, 195 (2009)
17. W.F. Krupke, M.D. Shinn, J.E. Marion, J.A. Caird, S.E. Stokowski, J. Opt. Am. B **3**, 102 (1986)